

Edge states induce boundary temperature jump in molecular dynamics simulation of heat conduction

Jin-Wu Jiang,¹ Jie Chen,¹ Jian-Sheng Wang,^{1,*} and Baowen Li^{1,2}

¹*Department of Physics and Centre for Computational Science and Engineering, National University of Singapore, Singapore 117542, Republic of Singapore*

²*NUS Graduate School for Integrative Sciences and Engineering, Singapore 117462, Republic of Singapore*

(Received 10 June 2009; published 7 August 2009)

We point out that the origin of the commonly occurred boundary temperature jump in the application of No se-Hoover heat bath in molecular dynamics is related to the edge modes, which are exponentially localized at the edge of the system. If heat baths are applied to these edge regions, the injected thermal energy will be localized thus leading to a boundary temperature jump. The jump can be eliminated by shifting the location of heat baths away from edge regions. Following this suggestion, a very good temperature profile is obtained without increasing any simulation time and the accuracy of thermal conductivity calculated can be largely improved.

DOI: [10.1103/PhysRevB.80.052301](https://doi.org/10.1103/PhysRevB.80.052301)

PACS number(s): 62.23.Kn, 44.10.+i, 65.80.+n, 02.70.Ns

Computer simulations of thermal transport are normally done by equilibrium and/or nonequilibrium molecular dynamics. In the latter approach, the experimental condition is mimicked by setting up temperature gradient across the system. The temperatures of two ends are kept fixed. No se-Hoover heat bath is one of the most effective approaches to realize constant temperature.^{1,2} As a generic phenomenon in existing works using No se-Hoover heat bath, a significant boundary temperature jump (BTJ) occurs between the temperature-controlled (TC) parts and the rest parts.³⁻⁶ This temperature jump is usually regarded as the consequence of thermal boundary resistance^{3,6} and it results in both larger calculation error and longer simulation time.

In this paper, we provide a sound physical explanation for the jump by relating it to edge modes (EM), which will be fully excited but localized on the boundary. Due to the EM, the thermal energy is localized if heat bath is applied to these edge regions (which means that the thermal current is injected into the system through these edge regions), leading to the boundary temperature jump. We then show that the temperature jump can be largely reduced by shifting the location of heat baths away from edge regions. This shift results in a better temperature profile and gives rise to a more accurate value of thermal conductivity. Our argument will be illustrated by the case study of heat conduction in different nanostructures such as nanoribbon, nanotube, and nanowire.

In our simulation, the second-generation Brenner interatomic potential is used.⁷ The Newton equations of motion are integrated within the fourth order Runge-Kutta algorithm, in which a time step of 0.5 fs is applied. The typical simulation time in this paper is 8.5 ns.

Figure 1(a) is the configuration of a graphene nanoribbon in our simulation. Each column contains four carbon atoms. There are 51 columns as shown in the corresponding schematic diagram Fig. 1(b). The outermost two black columns (1 and 51) are fixed. In vertical direction, periodic boundary condition is applied.

To study the thermal conductivity, we have to set up temperature gradient across the system and then calculate the thermal conductivity by Fourier's law. No se-Hoover heat

baths are applied to columns 2 and 50 with temperatures 310 and 290 K, respectively. 2×10^7 simulation steps (8.5 ns) are used for the system to reach thermal steady state. The difference between the thermal current from left and right heat baths, dJ , is used to determine whether the system has reached thermal steady state or not. In the steady state, dJ should be zero. Figure 2 shows that the system reaches thermal steady state after 2×10^7 steps where dJ is almost zero. The nonzero value of dJ is due to numerical errors and can be used to estimate the relative error of thermal conductivity as dJ/J , where J is the heat current through the system.

Figure 3(a) shows the temperature profile. The data are obtained by averaging over 8.5 ns after the steady state is achieved. This is a typical figure which also shows up in other existing works.^{3,5,6} It shows that the temperatures of the two TC parts are well controlled to be the required value. But an obvious jump occurs between the TC parts and the rest parts, i.e., between columns 2/3 on the left and columns 49/50 on the right. This jump cannot be removed by simply increasing simulation time and it leads directly to two negative effects. First, only temperatures in these columns far away from edges can be used to do linear fitting to get temperature gradient. The obtained value of temperature gradient is small (-5.5 K/ ) and sensitive to how many columns are chosen to do the linear fitting. So error in the temperature

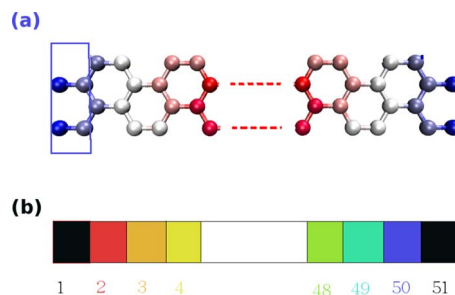


FIG. 1. (Color online) (a) Configuration for the graphene nanoribbon with length 106   and width 4.92  . (b) is a schematic figure for (a). It is periodic in the vertical direction. The two outermost columns (columns 1 and 51) are fixed.

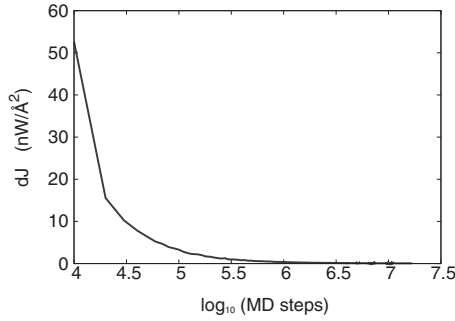


FIG. 2. The difference between the heat current flows from the left and right heat baths. The heat current is averaged over 8.5 ns in the thermal steady state. The horizontal axis is plotted in log scale.

gradient will be large. Second, the thermal current J is only $0.39 \text{ nW}/\text{\AA}^2$, which is also very small. As a result, longer simulation time is needed for the system to reach thermal steady state and the calculated value for thermal conductivity [$75.5 \text{ W}/(\text{mK})$] has large relative error estimated by $dJ/J = 14.3\%$.

To find an effective method to reduce this temperature jump, we first have to understand the underlying mechanism. Geometrically, the edge regions (columns 2/50) are very different from the other regions inside the system. They are in the edge of the system, where some eigenmodes' vibrational amplitude decreases to zero very quickly from edges into center. Figure 4 shows the normalized vibrational amplitudes in all six EM in this system, calculated from Brenner empirical potential implemented in "General Utility Lattice Program."⁸ It shows that the amplitudes decrease exponentially (red dotted fitting line) and these edge modes are doubly degenerate since they can be localized at either left or right edge regions (columns 2/50). Figure 5 shows explicitly that these EM have been excited. In Fig. 5, we do the Fourier transform for the vibrational amplitude of one atom in column 2. The other atoms in edge regions (columns 2 and 50)

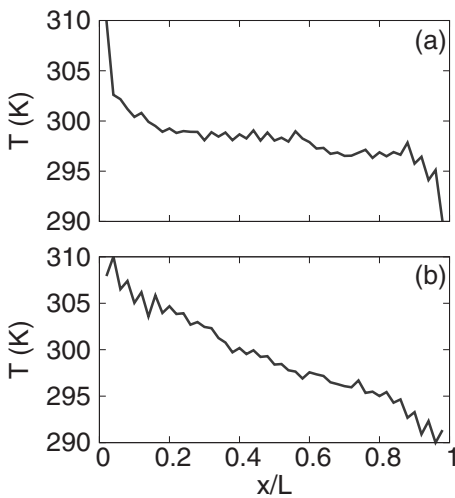


FIG. 3. Temperature profiles at 300 K for graphene nanoribbon, whose configuration is shown in Fig. 1. (a) Heat baths are applied to columns 2 and 50 (edge regions). (b) Heat baths are applied to columns 3 and 49 (away from edge regions). The data in both figures are obtained by averaging over 8.5 ns in the steady state.

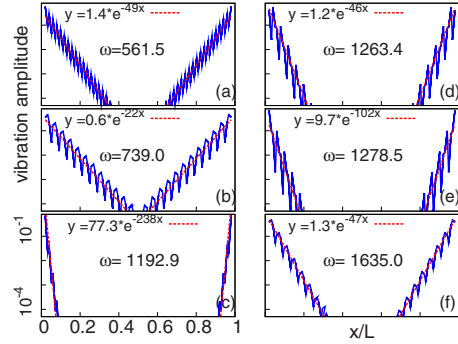


FIG. 4. (Color online) Normalized vibration amplitudes vs reduced x coordinate of each carbon atom. From (a) to (f) are six edge modes in graphene nanoribbon shown in Fig. 1. The frequency ω for each mode given in the figure is in cm^{-1} . The vertical axis is in log scale.

have similar results. Each peak corresponds to an excited phonon mode. We have denoted the six fully excited LEM in the figure. They are very important in two senses if the thermal current is injected through these edge regions: (1) in these modes, the vibration is localized at the edges, thus the thermal current will be localized, leading to small thermal current and small temperature gradient. (2) The total degrees of freedom in the TC part is 12 (4 atoms) only while there are six LEM. So the LEM have a very large component, as half of degrees of freedom in the TC parts are localized. Because of these two factors, large amount of thermal current is localized at the left and right edge regions. As a result, although the temperatures at the edges (columns 2/50) can reach the required value, there will be a big jump between TC parts and rest parts.

To reduce the temperature jump, one possible way is to increase the number of atoms in the TC region. So that the component of the EM will decrease relatively and the localized effect on the thermal transport will be suppressed. As a

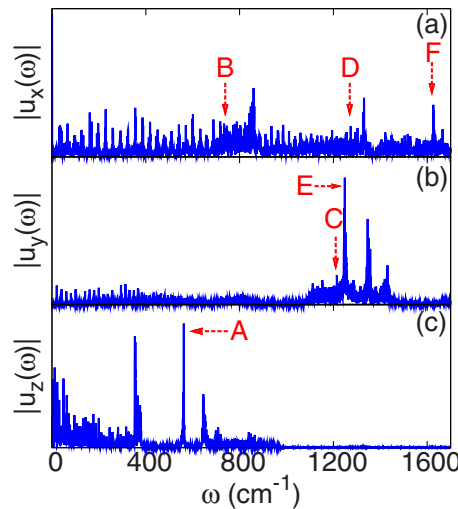


FIG. 5. (Color online) Fourier transform $\tilde{u}(\omega)$ of the vibrational amplitude $\tilde{u}(t)$ of the atom in the edge regions (columns 2 and 50). Labels A, B, C, D, E, and F denote the six corresponding localized edge modes in Fig. 4.

result, the jump will be reduced. The TC parts can be enlarged either in the vertical or longitudinal direction. However, we find that the number of EM will also increase if the TC part is enlarged in the vertical direction. Yet, this number is kept to be a constant if the TC part is enlarged in the longitudinal direction. So in this method, one can only enlarge the TC part in the longitudinal direction to reduce BTJ. It has been demonstrated that enlarging the system in the longitudinal direction has some effects on reducing the jump.³

Here we propose a more efficient method to solve this temperature jump problem. Due to the localization property of the EM, they are localized at the edge regions (columns 2/50) with the typical localization length as $L_{loc}=1$ column. We can therefore shift the location of heat baths to the regions where it is L_{loc} away from the boundary. Now we put columns 3 and 49 in the heat bath, instead of columns 2 and 50. In this way, the thermal current can be transported between TC parts (columns 3/49) and rest parts efficiently. We mention that the six EM in the edge regions are still excited in this situation. However, they cannot generate localization effect on the thermal current. Because now the thermal current is injected through columns 3 and 49. So we can achieve a very good temperature profile as shown in Fig. 3(b). The simulation time for this figure is the same as that in Fig. 3(a). Actually this temperature profile can be obtained within much shorter simulation time (4.0 ns) since the thermal current can now be injected into the system much more efficiently. We get a much larger temperature gradient -16.6 K/Å and larger thermal current 0.96 nW/Å². The obtained thermal conductivity is 61.6 W/(mK) with relative error $dJ/J=6.2\%$. This error is smaller than the previous one by a factor of 2. So following this proposal, one can calculate the thermal conductivity much more accurately by changing the location of heat baths away from the edge regions, which will not increase any simulation time.

Our explanation for temperature jump is actually independent of system. Because EM is essentially originating from the specific geometrical configuration of edge regions.⁹ This is similar to electronic- or spin-edge states.¹⁰⁻¹² To check the generality of our method, we apply it to reduce BTJ in single-walled carbon nanotube (SWCNT) and silicon nanowire (SiNW). The results are shown in Fig. 6. This figure confirms the applicability of our method. For SWCNT (5,0) with length 106 Å in this figure, we study the phonon modes in the system and find three LEM with frequency as 761.5 (double degenerate), 1331.5 (double degenerate), and 1416.0 (fourfold degenerate). Since there are fewer LEM in SWCNT, BTJ in this system is not very large even if heat baths are applied to edge regions. SiNW has a cross section of 3×3 unit cells (lattice constant 5.43 Å) and 10 unit cells in the longitudinal direction. Compared with the graphene nanoribbon or SWCNT, SiNW has a much larger BTJ if heat baths are applied directly to the edge regions. This is because of the high surface-to-volume ratio of SiNW. As a result, the number of EM is very large. We find 30 EM in this SiNW, which is the reason for large BTJ. This large BTJ can be reduced efficiently by changing location of heat baths away from edge regions to avoid the localization effect from EM (see Fig. 6). After the temperature jump is largely reduced,

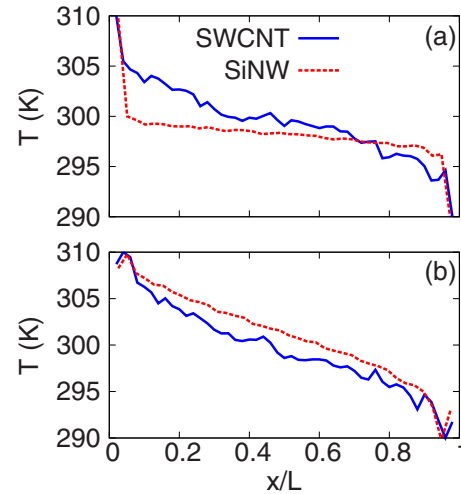


FIG. 6. (Color online) Temperature profiles for SWCNT (blue solid) and SiNW (red dotted). (a) Heat baths are applied to edge regions. (b) Heat baths are away from edge regions.

the temperature gradient and thermal current across the system are enhanced by about a factor of 7. So the thermal energy is efficiently pumped in, thus reducing simulation time, and the calculation error will be smaller by a factor of 7.

In conclusion, we have addressed a very generic problem—the boundary temperature jump in molecular dynamics simulation of heat conduction. We have provided strong evidence that this jump is related to the EM, which are localized exponentially in the edge regions. These modes will localize thermal current if heat baths are applied exactly to these edge regions, leading to BTJ. An effective way to reduce BTJ is to shift the location of heat baths away from edge regions. In this way, the thermal current can be transported between TC parts and rest parts efficiently and a better temperature gradient can be established. Therefore, thermal conductivity can be calculated much more accurately without increasing computation time.

We have five further remarks: (1) here we consider Noé-Hoover heat bath to illustrate that EM take the responsibility for temperature jump. Actually, this explanation is also valid when other heat bath is applied. Because the essential function of heat bath is to excite all phonon modes in the TC part, including localized modes. So in the case of other kind of heat bath, temperature jump also occurs if heat bath is applied exactly to the edge regions. Due to its randomness property at each step, the Langevin heat bath can suppress some of the accumulation effect of EM. So BTJ in Langevin is generally smaller than that in Noé-Hoover heat bath.¹³ (2) In this paper, we use fixed boundary condition in the longitudinal direction. For free boundary condition, we also find eight doubly degenerate EM with frequency as 97.3 , 244.4 , 473.4 , 516.5 , 1379.3 , 1634.4 , 1697.7 , and 1703.0 cm⁻¹. These modes are localized at columns 1 and 51, which are edge regions in free boundary condition. In this case, the number of EM is increased and the frequencies for the first four are lower. So the localization effect will be more serious if heat baths are applied to the edge regions (columns 1 and 51), resulting in even larger BTJ.⁵ BTJ in this situation can

also be removed by changing the location of the heat baths away from the edge regions. For periodic boundary condition, the EM turn into optical phonon modes in the system. The velocity of optical-phonon modes is very small, which will also have “localization” effect on the thermal current, leading to big BTJ.¹⁴ This BTJ can be reduced by artificially confining the injected thermal energy to acoustic phonon modes.¹⁵ However, practically it is more complicated since the injected phonon should follow the Bose-Einstein statistics if the thermal conductivity is studied. (3) In experiments, these EM will also be excited if the heat source or sink is located exactly in the edge regions, leading to smaller thermal current and smaller temperature gradient. As a result, experimental errors increase. So it is important to put heat source and sink away from the edge regions to avoid the thermal current being localized. (4) BTJ can be removed by enlarging TC parts in the longitudinal direction as in Ref. 3 or by changing location of heat bath as in this paper. Actually

there is a small remaining BTJ in both results [Fig. 2 in Ref. 3 and Figs. 3(b) and 6(b) in this paper]. This small BTJ is the result of thermal boundary resistance between TC parts and rest parts. How to remove this small remaining BTJ is still a problem and requires further investigation. (5) The EM discussed in this paper has some similar to the Rayleigh waves,¹⁶ which is confined to travel across surfaces of solids. The wave velocities of Rayleigh waves are slow, leading to some localization effect. Yet, the penetrate depth of Rayleigh is approximately equal to the wavelength, which is larger than that of the EM (typically $L_{\text{loc}} \approx 1$ column, in Fig. 4).

We thank Pawel Koblinski for helpful comments, and Xiang Wu and Nuo Yang for useful discussions. The work is supported by a Faculty Research Grant No. R-144-000-173-101/112 from NUS, Grant No. R-144-000-203-112 from the Ministry of Education of the Republic of Singapore, and Grant No. R-144-000-222-646 from NUS.

*Corresponding author. phywjs@nus.edu.sg

¹S. Noše, *J. Chem. Phys.* **81**, 511 (1984).

²W. G. Hoover, *Phys. Rev. A* **31**, 1695 (1985).

³J. Shiomi and S. Maruyama, *Jpn. J. Appl. Phys.* **47**, 2005 (2008).

⁴M. C. H. Wu and J. Y. Hsu, *Nanotechnology* **20**, 145401 (2009).

⁵G. Zhang and B. Li, *J. Chem. Phys.* **123**, 114714 (2005).

⁶S.-C. Wang, X.-G. Liang, X.-H. Xu, and T. Ohara, *J. Appl. Phys.* **105**, 014316 (2009).

⁷D. W. Brenner, O. A. Shenderova, J. A. Harrison, S. J. Stuart, B. Ni, and S. B. Sinnott, *J. Phys.: Condens. Matter* **14**, 783 (2002).

⁸J. D. Gale, *J. Chem. Soc., Faraday Trans.* **93**, 629 (1997).

⁹S. Y. Kim and H. S. Park, *Nano Lett.* **9**, 969 (2009).

¹⁰M. P. Lima, A. Fazzio, and A. J. R. da Silva, *Phys. Rev. B* **79**, 153401 (2009).

¹¹L. Yang, M. L. Cohen, and S. G. Louie, *Phys. Rev. Lett.* **101**, 186401 (2008).

¹²A. Bermudez, D. Patane, L. Amico, and M. A. Martin-Delgado, *Phys. Rev. Lett.* **102**, 135702 (2009).

¹³J. Chen, G. Zhang, and B. Li (unpublished).

¹⁴P. K. Schelling, S. R. Phillpot, and P. Koblinski, *Phys. Rev. B* **65**, 144306 (2002).

¹⁵Pawel Koblinski (private communication).

¹⁶L. Rayleigh, *Proc. Lond. Math. Soc.* **s1-17**, 4 (1885).